Inspection of Weld Bead using High Speed Laser Vision Sensor

H. Lee, S. Ahn, K. Sung and S. Rhee

Abstract

Visual inspection using laser vision sensor was proposed for fast and economic inspection and was verified experimentally. Welding is one of the most important manufacturing processes for automotive and electronics industries as well as heavy industries. The weld zone influences the reliability of the products. There are two kinds of weld inspection tests, destructive and non-destructive test. Even though the destructive test is much more reliable, the product should be destroyed, and hence the non-destructive test such as ultrasonic or X-ray test was used to overcome this problem. However, these tests are not used for real time inspection.

Key Words : High speed laser vision sensor, Real time visual inspection, Welding, Image processing.

1. Introduction

In this study a high-speed laser vision system and a real time visual inspection algorithm was developed in order to visually inspect the welding part at real time.

The welding inspection is an essential part of the manufacturing process. However inspection for all parts by X-Ray or ultrasonic is impassible in mass production. Thus most welding part inspections are visual test done by the naked eye. Inspections preformed by humans are subjective and is not quantitative. Therefore an automatic impartial inspection test is needed for productivity and quality improvements. [1-4]

A laser vision sensor was used as it can receive accurate information about the exact distance. R. J. Barnett[5] et al. used a CCD camera to acquire 2-dimensional images and then calculated the intensity of the width and the length of the welding bead??s ripple to decide the weld quality[6,7]. Soudronic company inc. of Switzerland used a laser vision sensor MVS-10 that projected 5 beams simultaneously to decide the welding shape of a tailored blank welding, a CCD camera that acquired 2-dimensional images and then the seam concavity, seam convexity, misalignment, bead width, and the lack of penetration were calculated and the welding flaw was decided. Y. S. Kim [8]used a laser vision sensor to measure the welding bead form and used artificial neural network to find the welding bead visual flaw.

The laser vision sensors used in the existing study can detect a maximum of 30 range data. In this study, in order to inspect at real time, 100 range data per second in needed at the least. Therefore a CCD that can capture more than 100 images per second was used. Image processing time was also reduced from the existing 30msec to 10msec. The conventional image processing method was improved for a faster result.

H. Lee and ***K. Sung*** : Dept. of Precision Mechanical Engineering, Hanyang University, Seoul, Korea
E-mail : manian21@hanyang.ac.kr
S. Ahn : Department of Train Operation & Mechatronics, Korea National Railroad College, Kungki-Do, Korea
E-mail : shahn@chuldo.krc.ac.kr
S. Rhee : School of Mechanical Engineering, Hanyang University, Seoul, Korea
E-mail : srhee@hanyang.ac.kr

2. Image processing

In the productivity line applied in this study, it must not take more than 8 seconds to inspect 1 product. The loading and unloading of the product takes 1.5 seconds, which leaves the actually testing time at 6.5 seconds. Within the testing time, 1.5 seconds must be used to distinguish the welding defect part, and the remaining 5 seconds must be used to obtain the form of welding. In order to acquire the precise shape within the 5 seconds, at least 90 range data pre second must be obtained and a CCD camera that obtains 100 images per second was used. As 100 images per second is obtained, the image processing time in limited to 10ms.

The conventional image processing method obtains range data and eliminates the noise component by covering several steps. The image processing time takes 26.27msec on average. This study improves the original algorithm and by covering the average filter, thresholding, thinning and profiling, the entire image processing time can be reduced to 9.23msec on average. The image size used in the inspection system is 530 by 430 pixels

Table 1 Compare image processing time (msec)

	Conventional image processing	Proposed image processing
Filtering	14.5	5.85
Thresholding	3.56	
Thinning	4.86	1.36
Profiling	3.35	2.02
Total	26.27	9.23

2.1 Median filter and thresholding

By thresholding the images from the beginning, two effects ; eliminating the noise of the small component and reducing the general calculation amount were realized concurrently.

The filtering and thresholding section reduced the image processing time the most. The proposed algorithm used in this study reduced the calculation amount by more than half, so the time could be reduced.

$$I_{new}(X,Y)=\begin{cases}255 & : if \sum_{Y-m}^{Y+m}\sum_{X-n}^{X+n} I_{raw}(X,Y) > T_{thres} \\ 0 & : otherwise\end{cases} \quad (1)$$

Fig. 1 Original image

Thresholding and filtering was simplified as shown in Eq. 1, to reduce the calculation time. However from Fig. 2 (a) and (b), it is shown that more noise is formed compared to the conventional processing, thus the noise element is eliminated after the profiling operation.

2.2 Thinning

The thinning algorithm used in this study is a method that selects the middle point of the continuous laser line from a vertical direction. Even though there is several laser elements in a vertical direction, each middle point of each section in marked. Unlike before, noise was remained after the thinning method but the processing time was reduced by 1/3.

2.3 Profiling

After thinning processing, the image still has both noise and laser line components. The laser line shows that is has a continuous curved line. On the other hand, the noise element shows discontinuity and a large difference in the average amount. With these distinctive features, an algorithm shown in Fig. 2 was

(a) Conventional method (b) Proposed method

Fig. 2 Image after filtering, thresholding, thinning

developed. When only 1 middle point exists in each pixel rows, this becomes the fixed point. But if there are more than 2 middle points, the profiling algorithm is used to find the fixed point.

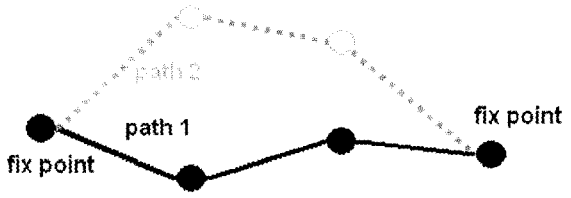

Fig. 3 Diagram of the shortest path algorithm

$$\mathrm{Len}_{\mathrm{path}} = \sum_{i=1}^{n-1} \sqrt{(x_i - x_{i-1})^2 + (y_i - y_{i-1})^2} \quad (2)$$

$$\mathrm{Len}_{\mathrm{path}} = \sum_{i=1}^{n-1} |(y_i - y_{i-1})| \quad (3)$$

When the fixed point is selected, the gathering of points with the shortest distance is chosen. The equation to find the distance is shown in Eq. (2). This is an operation that takes a very long time. When choosing the path, the relative length is enough than the actual length, thus Eq. (3) can be used. Through this profiling process, the noise was successfully eradicated after the thinning process.

2.4 Result of image processing

The conventional algorithm was simplified to obtain a three times faster operation speed. Also, in order to obtain the same accuracy as the conventional algorithm, a profiling algorithm was developed. As shown in Fig. 4. The accuracy of the image processing data showed the same results as the conventional method, with an average of 0.547 pixel error.

3. Procedure of experiment

In this study, shock absorbers of automobiles were inspected welding defect using high speed laser vision sensors. Shock absorber has four inspection parts. These parts were inspected by four laser vision system at the same time.

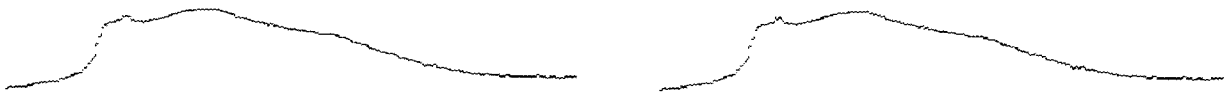

(a) Conventional method (b) Proposed method

Fig. 4 Result of image processing

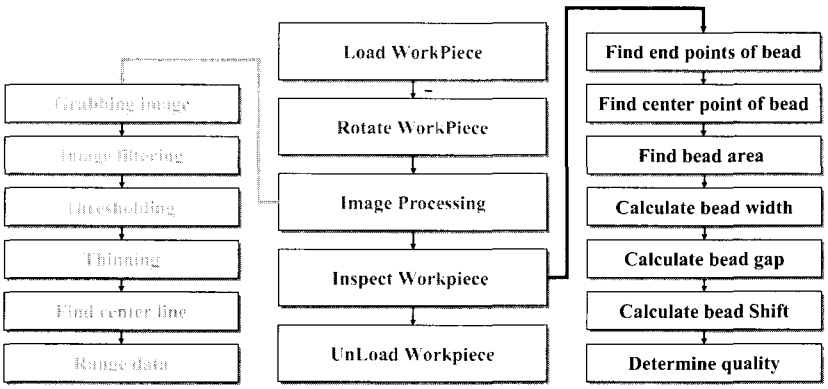

Fig. 5 Flow chart of bead inspection using laser vision sensor

Laser vision inspection system was organized with 4 clients and 1 server. Server connected with four clients by TCP/IP network. A client inspects a part of shock absorber, and server collects results inspected by client. Server displayed the results of inspection, and was connected PLC (programmed logic controller). So it has functions of sending the signal of start and end inspection to PLC.

Laser vision sensor generated the distance data after workpiece was moved on the work place by robot and was started to rotate. And defect inspection was started with the distance data. Clients sent the test results to the server, and the server sends the result the final results by using the sent result from client to the PLC. Robot classified acceptable workpiece and unacceptable workpiece by the final result. The real time defect inspection was processed repeatedly as this order.

4. Configuration of experiment equipments

Fig. 6 shows the shock absorber and the weld bead that this image processing algorithm applied for inspecting. The system developed in this study uses 4 sensors to find 12~15 visual defects of 36 different parts.

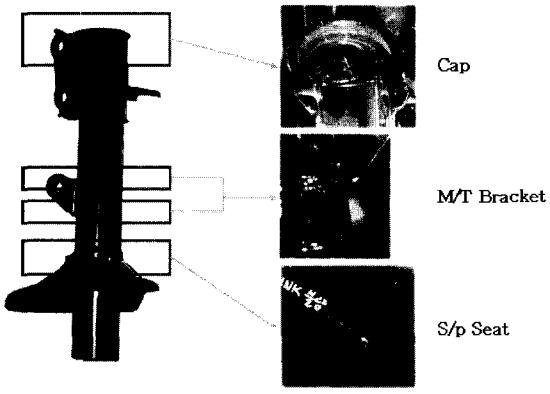

Fig. 6 Laser line shape for each bead part

4.1 Defect of bead width

The welding defect of the bead width defect has many reasons, such as inadequate input current, arc instability, and inaccurate mechanism etc. Fig. 7 (a) shows the cap image of the shock absorber. Fig. 7 (b) shows the spring seat image of the shock absorber. The slope method from the range data is used to abstract feature point results, and this is shown in each figure. In each picture, the left red point and the middle to left blue point shows each end point of the bead.

The calculated end point interval of the bead, thus the width, is used to find the bead width defect. Fig. 8 is a graph that shows the bead width change of Fig. 7 (a).

When the welding bead width is within the maximum

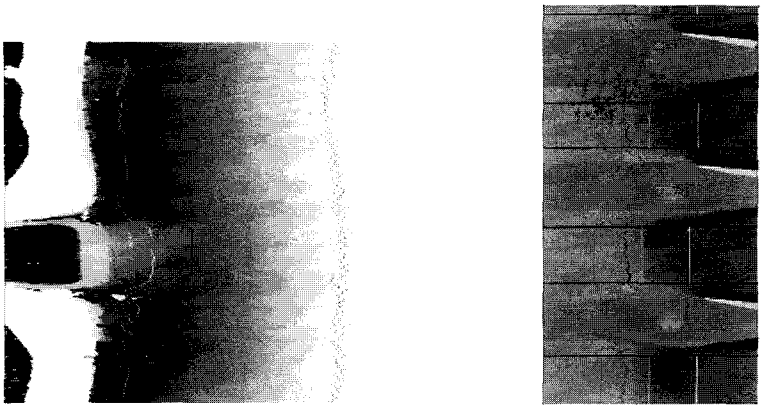

(a) Cap (b) Seat

Fig. 7 Range image

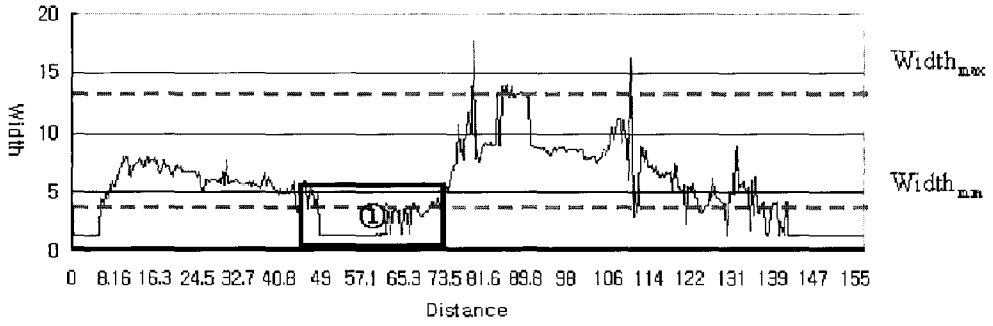

Fig. 8 Variation of measured bead width on cap (unit: mm)

and minimum range, it is assumed as fair bead, if not in the range, it is assumed as defective bead. The defect area is area ①. The width and length of the area that is out of the range are used as to detect the defect.

In Fig. 8, both of boundary lines show the maximum and minimum of the weld bead width.

4.2 Defect of bead shift

Weld bead shift is usually occurred in seat part. During the bead shift, the robot weld cannot find the exact position for automatic welding. This defect allows the bead to be produced at an abnormal position. The shifted weld bead is located at wrong place. The cross section of this bead shapes a valley. Two points, found to be the bead end point, are joined by a straight line, and the area of the range below the line is found. It is assumed that this dimension of region is the rate of the shift, as shown in Fig. 9.

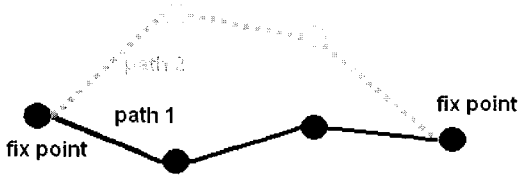

Fig. 9 Calculation of bead shift region

Fig. 8 shows the range data of the weld bead, which has defeat of bead shift on seat and the change of its value at a cylinder direction. Fig. 10 (b) is the graph that shows the change of measured bead shift performed in Fig. 10 (a).

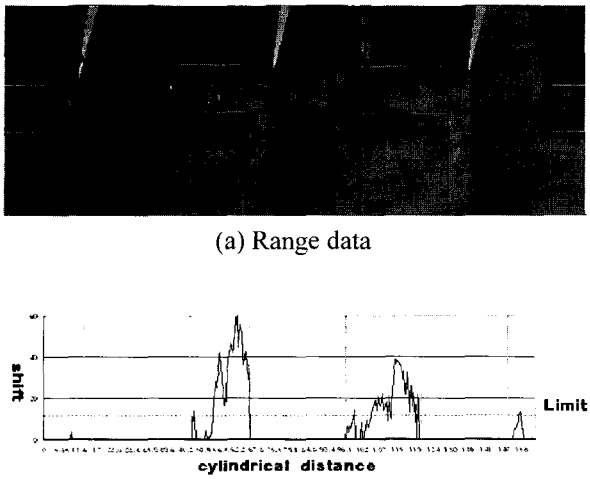

(a) Range data

(b) Variation of measured bead shift on seat

Fig. 10 Seat image

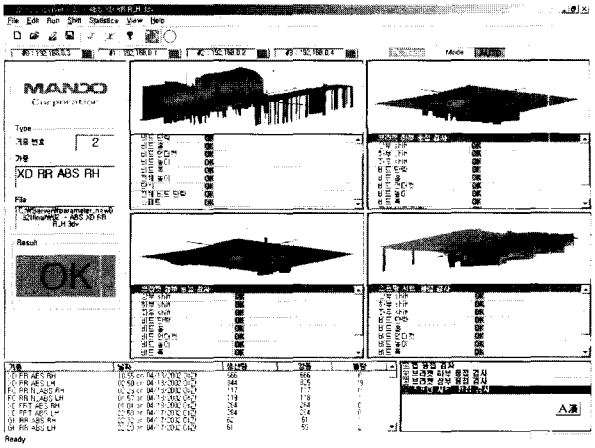

Fig. 11 Server program displayed the result of inspected welding bead

4.3 Result of weld bead visual inspection

The developed system reduces the image processing time and the welding defect detecting time, by using private controllers for each 4 inspection part. Fig. 11 shows the inspection result of the distance information found by each controller and the defect information transmitted to the central server through the TCP/IP.

The image-processing algorithm loaded on each controller and the defect algorithm is optimized to be compatible at each testing part. The inspection algorithm is developed to out stand exterior noise generation and one-sided rotation. Also, it is shown that minute defects do not effect to the final results.

The inspection system developed in this study can test more than two hundred thousand welding beads in a day. On average approximately about 20 out of 3000 is shown to have defects, but the actual defect rate is 50%. However, there has been no record so far about defects from those that are tested to be good.

5. Conclusion

The developed image processing algorithm in this study simplified the conventional algorithm, and excluded the multiple and divisional operation in the computer equation to reduce the time. The profiling method was added to keep the same accuracy as the conventional system.

High-speed laser vision system and a real time visual inspection algorithm were developed in order to visually inspect the welding part at real time. This system can inspect all products at real time without destructing the product. Also, this system can finish all tests of one product within 5 seconds, and can determine if the product is a defect with an error of less than 0.2%.

Acknowledgements

This work was supported by Hanyang University in 2000.

References

1. K. Kugai, S. Muto, and T. Mouri : The development and application of welding robot control technique using laser vision sensor, *Welding Technology*, Vol. 46, No. 5 (1998), pp. 105-110
2. P. Kim and S. Rhee : Automatic teaching of welding robot for free-formed seam using laser vision sensor, *Optics and Lasers in Engineering*, Vol. 31 No. 3 (1999), pp. 173-182
3. Z. Smati, D. Yapp, and C. J. Smith : Laser guidance system for robots, Robotic welding, *Springer-Verlag*, (1987)
4. Y. Suga and A. Ishii : The image processing application for welding process control and automatic welding qualification, *The International Journal of Japan Society Precision Engineering*, Vol. 32, No. 2 (1998), pp. 81-84
5. R. J. Barnett, G. E. Cook, A. M. Strauss, K. Anderson, and J. F. Springfield : A vision based weld quality evolution system, Trends in Welding Research, *Proceedings of the 4th International Conference*, June (1995), pp. 689-694
6. R. C. Gonzalez and R. E. Woods : Digital image processing, *Addison Wesley*, (1993)
7. R. Jain, R. Kasturi, and B. G. Schunck : Machine vision, *MIT Press and McGraw-Hill*, (1995)
8. Y. S. Kim : A study of inspection of weld bead defects using artificial neural network, *Master Thesis*, Hanyang University, (1998)